Supporting Information

Tuning Hydrocarbon Selectivity in Electrochemical CO_2 Reduction via Copper-Porphyrin Immobilization on Carbon Nanotubes

Alaleh Esfandiari[1], Maryam Abdinejad* [2,3], and Ali Seifitokaldani*[1]

[1]*McGill University, Department of Chemical Engineering, Montreal, Quebec, Canada*
[2] *Massachusetts Institute of Technology, Department of Chemical Engineering, 02139 Cambridge, MA, USA*
[3]*Technical University of Denmark, Department of Energy Conversion and Storage, Fysikvej, 2800 Kgs Lyngby, Denmark*

Number of Pages: 15

Number of Figures: 13

Number of tables: 2

Contents

Reagents and Chemicals

All chemicals and solvents of commercial reagent grade listed in this section. Chloroform (> 99.8 %D), Nafion™ perfluorinated resin solution (5 wt. % in mixture of lower aliphatic alcohols and water), N,N-Diisopropylethylamine (DIPEA)(≥99%) Deuterium oxide (D_2O) 99.9 atom % D, N,N-Dimethylformamide (DMF)(≥99%), Copper (II) sulfate pentahydrate ($CuSO_4.5H_2O$) (≥98%), Dichloromethane(DCM)(99.8%) and Ethanol purchased from Sigma-Aldrich. l5,10,15,20-Tetrakis(4-methoxycarbonylphenyl)porphyrin(>95.0%), Carbon Nanotube Multi-walled (MWCNTs) (10-20nm (diam.), 5-15micro m(length)), were purchased from TCI America. Dimethyl sulfoxide (DMSO) purchased from ACP chemicals. Reverse osmosis water was generated by a MilliQ (resistivity 18.2 MΩ .cm) system.

Synthesis Method

Preparation of copper tetraphenylporphyrin (TMCPP): $CuSO_4.5H_2O$ (0.3 mmol) and *N,N*-Diisopropylethylamine (DIPEA) (0.051 mL) were added to a solution of porphyrin (0.06 mmol) in chloroform and 1/3 portion of ethanol. The reaction mixture was stirred for 2 h at the reflux of solvent at 60 ^oC. Subsequently, the mixture was allowed to cool down, and the solid crude complex was washed with chloroform and distilled water three times under vacuum filtration and let it dry overnight under vacuum. The powder was heated under 80 ^oC for 2hr in the oven to remove any residue.

Preparation of immobilized porphyrins onto carbon nanotubes: porphyrin compounds (20 mg) was dissolved in DMF (2 mL) and sonicated for 30 min. Then added to the mixture of CNTs (10 mg) and DMF (2mL) and sonicated for another 30 minutes to achieve a uniform suspension. The whole mixture was stirred at room temperature overnight. 20 µL of Nafion as a binder was added to the resulting suspension. Next, 400 µL of the resulting suspension was then drop casted on the carbon paper surface of 1.6*1.6 cm^2 and let it to dry for 24 hours. For 0.6 cm diameter glassy carbon surface, 20 µL of solution were drop casted to utilize in H-cell. The same procedure was used for the synthesis of Cu-TMCPPCNT mixture but instead of DMF, ethanol was used for drop casting solution. [1–4]

Advanced Characterization

To confirm successful synthesis of copper porphyrin Ultraviolet–visible spectroscopy UV-vis spectroscopy using Dichloromethane (DCM) as a solvent was used. Mass Spectrometry (MS) was conducted in Bruker Daltonics flex. Visualization of porphyrin done by Mercury software.

The morphology and composition of the catalyst on a carbon-Gold 150 mesh Grid have been analyzed using high- resolution transmission electron microscopy (TEM) (Talos F200X G2 S/TEM) with Single tilt beryllium low background holder to avoid any copper signal from holder. The elemental mapping was determined using energy-dispersive X-ray spectroscopy (EDX).

Atomic force microscopy MFP3D AFM equipped with a molecular force probe controller (Asylum Research – Oxford Instruments, Santa Barbara) was performed on a Cu-TMCPP deposited on silicon to investigate the thickness of Cu-TMCPP. Data processed using MountainsSPIP v. 10.1.10606 (Digital Surf, Besançon, France).

Single crystal X-ray diffractometer (XRD) was performed using the Bruker D8 Venture. V. For XRD simulation Mercury and VESTA software was used. X-ray photoelectron spectroscopy (Thermo-Scientific, K-Alpha XPS apparatus) at the Cu K-edge source used to investigate chemical and electronica state of the catalyst. Spot size used was 400 µm. Advantage software was used for data analysis and C1s peak at 284.8 eV considered as a reference. The X-ray absorption spectroscopy (XAS) performed at Canadian Light Source (CLS) was utilized for total electron yield (TEY) and fluorescence yield (FY) modes. In this research FY measurements were considered to have a stronger signal. The Extended X-ray Absorption Fine Structure (EXAFS) analysis was performed in the ATHENA software package. The structural parameters such as coordination number and bond distance reported from fitting of the first shell through Artemis software. In-situ XAS experiments performed in ambient using electrochemical flow-cell with the Soft X-ray Micro-characterization Beamline (SXRMB). (SI3) Catalyst was drop casted on a carbon paper substrate for both Ext-situ and In-situ XAS and Copper foil, Cu_2O and CuO powder representing (Cu^0) ,(Cu^{1+}) and (Cu^{2+}) respectively used as reference for calibration and linear combination fitting in this experiment.

Electrocatalytic CO_2 Reduction Performance

Electrocatlytic experiments were performed using both H-cell and custom-built three-chamber flow-cell electrolyzer. SI Ag/AgCl electrode (3 M KCl, Sigma Aldrich) and nickel foam or platinum plate (Corrtest Instruments Co.) used as reference electrode and counter electrode respectively. The anion exchange membrane used was Fumasep (Fumatech).The Anolyte and catholyte were 0.5 M KOH and $KHCO_3$ (Sigma Aldrich) circulated through the anodic and cathodic chambers with a flow rate of 5 ml/min respectively. Fundamental Electrochemical evaluations such as linear sweep voltammetry (LSV), cyclic voltammetry (CV), and electrochemical impedance spectroscopy (EIS) were performed in H-cell in which catalyst deposited on the Glassy carbon with 0.6 cm diameter and platinum plate served as counter electrode. While Electrocatalytic performance evaluations was performed in the sealed flow-cell with three-electrode configuration with nickel foam as counter electrode. The working electrode substrate was a gas diffusion carbon paper (YLS- 30T) to drop cast Cu porphyrin catalyst material. Continuous of CO_2 purged through the gas chamber within the flow rate of 30-40 ml/min. All electrochemical measurements were implemented using an Autolab potentiostat. All potentials reported with respect to the reversible hydrogen electrode (RHE) using following equation:

$E(RHE) = E(Ag/AgCl) + E_0(Ag/AgCl) + 0.059\times pH + 0.95\ IR$

IR compensation factor =0.95

The Ohmic resistance was measured using the electrochemical impedance spectroscopy (EIS) with an amplitude of 50 mV from 10^{-1} to 10^{6}. In constant-potential (CP) measurement each experiment run for 45 minutes, and 3 GC injection were analyzed for each potential.

CO_2 Reduction Reaction products Analysis

Gas products were analyzed in 1mL volume via in line Gas chromatography (a Clarus 590 GC with dual columns HayeSep N column and MoleSieve 13X column). The gas outlet of the flow-cell was connected to the GC instrument using copper tubing and gas-tight connectors. Argon used as a carrier gas in GC. The thermal conductivity detector (TCD) used for CO and H_2 and Flame Ionization Detector (FID) with a methanizer was used for C_2H_4 and CH_4 quantification. Calibration for each detector was done by a standard gas cylinder. The liquid products were analyzed using nuclear magnetic resonance (1H NMR) spectroscopy 0.45 g of the acidified solution was mixed with 0.15 g of D_2O containing 0.1 %DMSO as the locking solvent and the reference Respectively. Chemical shifts were reported in ppm and MestReNova software used for data processing.

Faradaic Efficiency (FE) in percentage was calculated for both gas and liquid products using following equation:

$$\text{FE} = \frac{Q\ experimental}{Q\ theoritical}$$

$$\text{FE} = \frac{n \times z \times F}{Q}$$

Q : the charge in Coulombs (C),

z :is the number of electrons to produce product,

(For example: 6 electron need for reduction for CO_2 to CH_4),

n : number of moles of products,

F : Faraday constant (96500 C/mol).

The reported FE are averaged values of 2 separate drop casted catalysts with measurements from three individual gas injection runs at each potential.

In this research, the Turnover Number (TON) and Turnover frequency (TOF) was calculated based on the equations bellow:

$$\text{Turnover Number (TON)} = \frac{mol\ of\ products}{mol\ of\ catalyst}$$

$$\text{Turnover frequency (TOF)} = \frac{TON}{t}$$

“mol of products“ refer to hydrocarbon products produced in electrolysis,
“mol of catalyst” calculated by the total deposited catalyst’s concentration on electrode,
“t” refers to time of reaction.

The TOF calculated based on the total deposited catalyst’s concentration on electrode which is a method that underestimates the activity of the catalyst.[4–6]

The double layer capacitance (Cdl) was evaluated by cyclic voltammetry (CV) at non-Faradic region with different scan rate using following equation:

$$C\text{dl} = \frac{\Delta j\ (ja - jc)}{2\nu}$$

ν: The scan rate in mVs^{-1},

ja : anodic current densities,

jc : cathodic current densities,

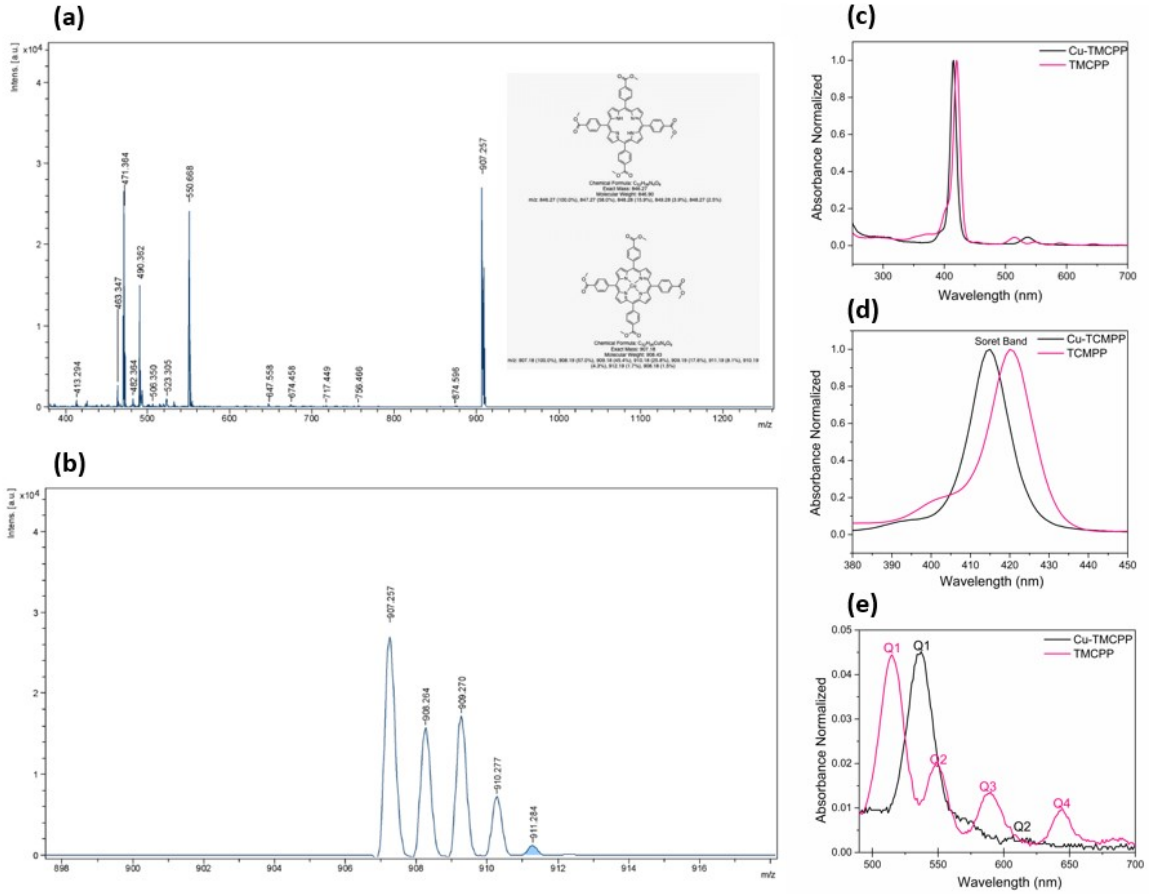

Fig. S1. (a) Mass spectrometry of Cu-TMCPP. (b) High-Resolution Mass Spectrometry of Cu-TMCPP. (c) UV-Vis spectroscopy showing Soret band and Q bands of porphyrin (TMCPP) and Cu-TMCPP. (d) High magnification of Soret band of porphyrin (TMCPP P) and Cu-TMCPP (e) High magnification of Q bands of porphyrin (TMCPP) and Cu-TMCPP.

The reaction progress of metalation of porphyrin with Copper (II) was monitored by UV-vis spectroscopy. The insertion of copper into porphyrin has been confirmed by the Soret peak blue shift from 420 nm to 414 nm. In addition, for porphyrin molecule there are four Q bands appeared around 514 nm, 550 nm, 590 nm and 643 nm, while by insertion of metal and coordination of Cu with N and removal of two protonated inner nitrogen atoms, there are just two peaks at 537 nm and 617 nm due to the more symmetrical structure.[2,6,7]

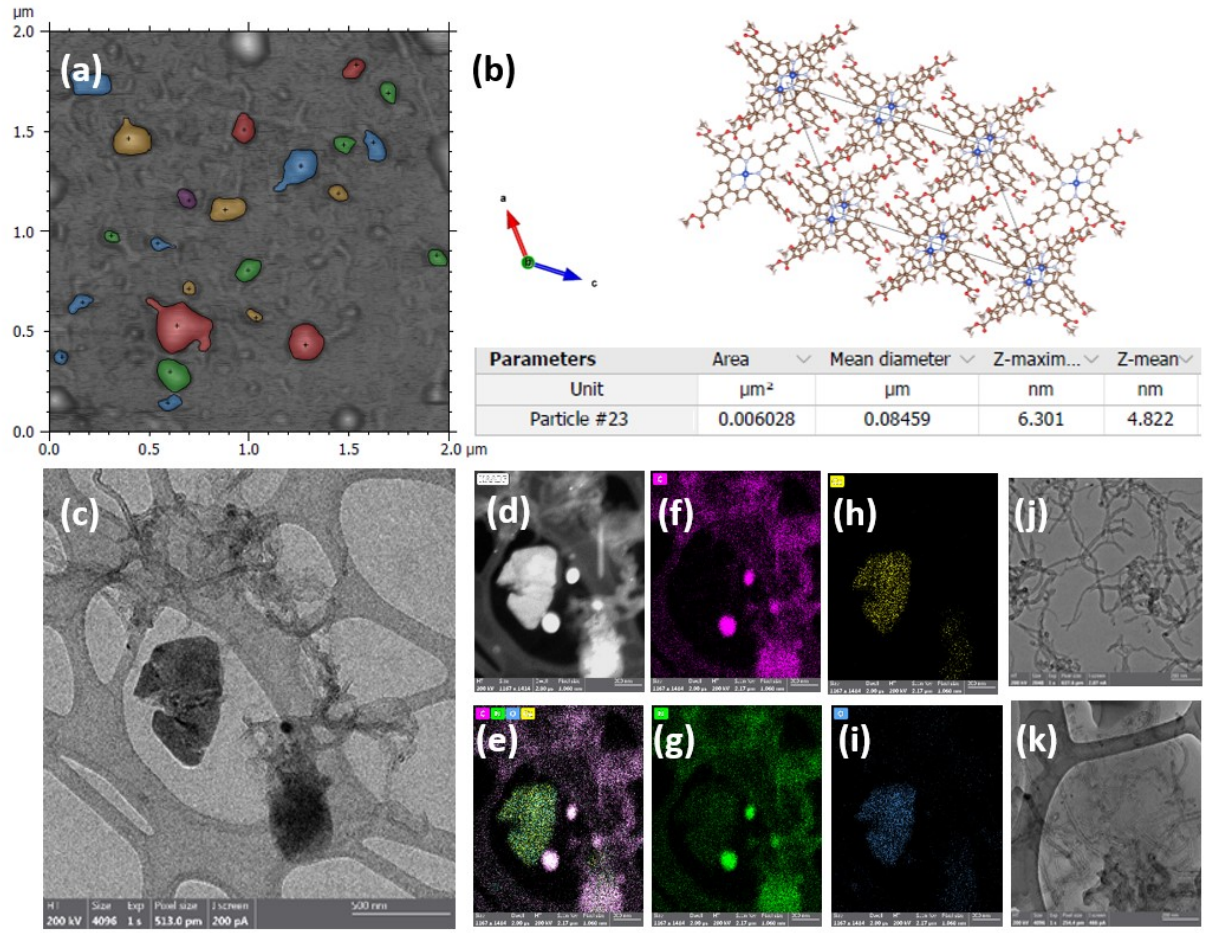

Fig. S2. (a) Average thickness of 23 particles were calculated to be 4.822 nm via AFM analysis of Cu-TMCPP. (b) Cu-TMCPP structure using VESTA visualization software has been reported to have plane distance of 8.9 Å inside one unit cell [8]. (c) Cu-TMCPP + CNT TEM. (d and e) Cu-TMCPP + CNT elemental mapping of (f)

carbon, (h) copper, (g) nitrogen and (i) oxygen. (j) High- resolution transmission electron microscopy (HR-TEM) comparison of bare CNT and (k) Cu-TMCPP/CNT showing the immobilized Cu-TMCPP on CNT.

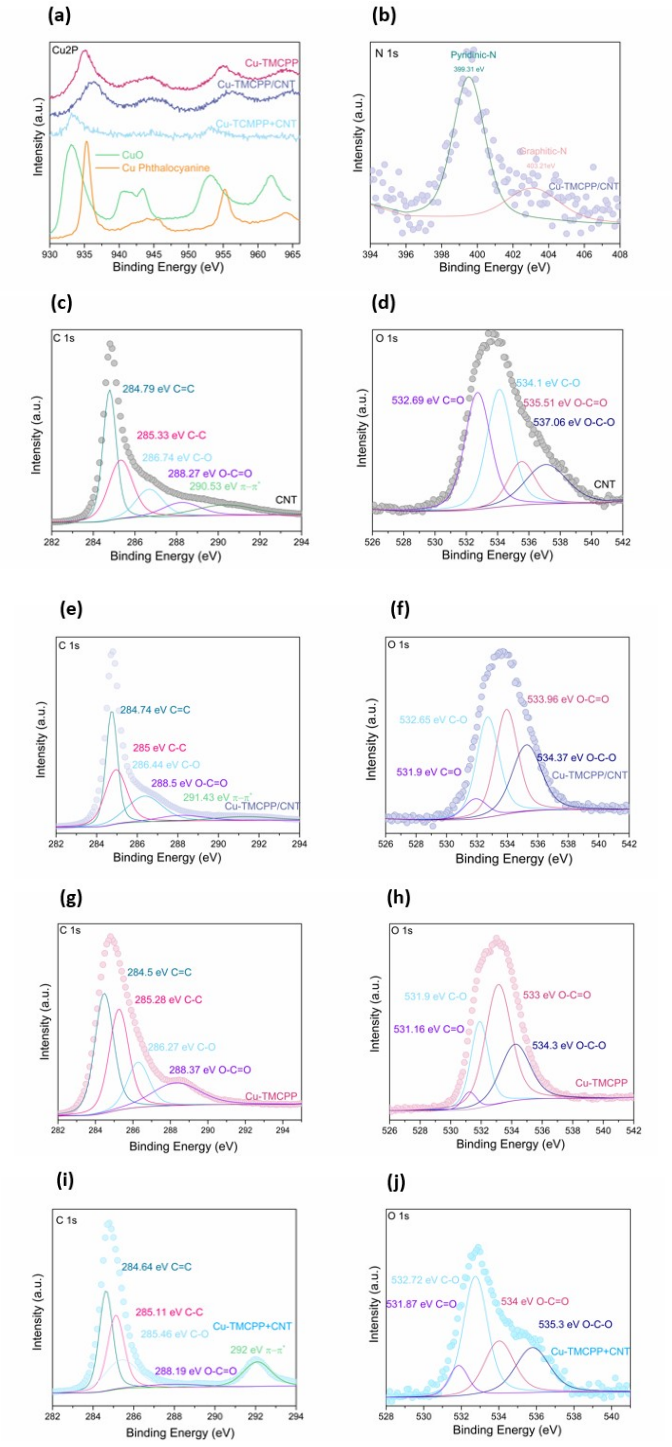

Fig. S3. (a) XPS survey for Cu-TMCPP, Cu-TMCPP/CNT, Cu-TMCPP + CNT , CuO and Cu phtalocycnine reference. (b) XPS spectra of N 1s for Cu-TMCPP/CNT. (c) C 1s and (d) O1s of Cu-TMCPP/CNT. (e) C 1s and (f) O 1s of Cu-TMCPP. (i) C 1s and (j) O 1s of Cu-TMCPP + CNT.

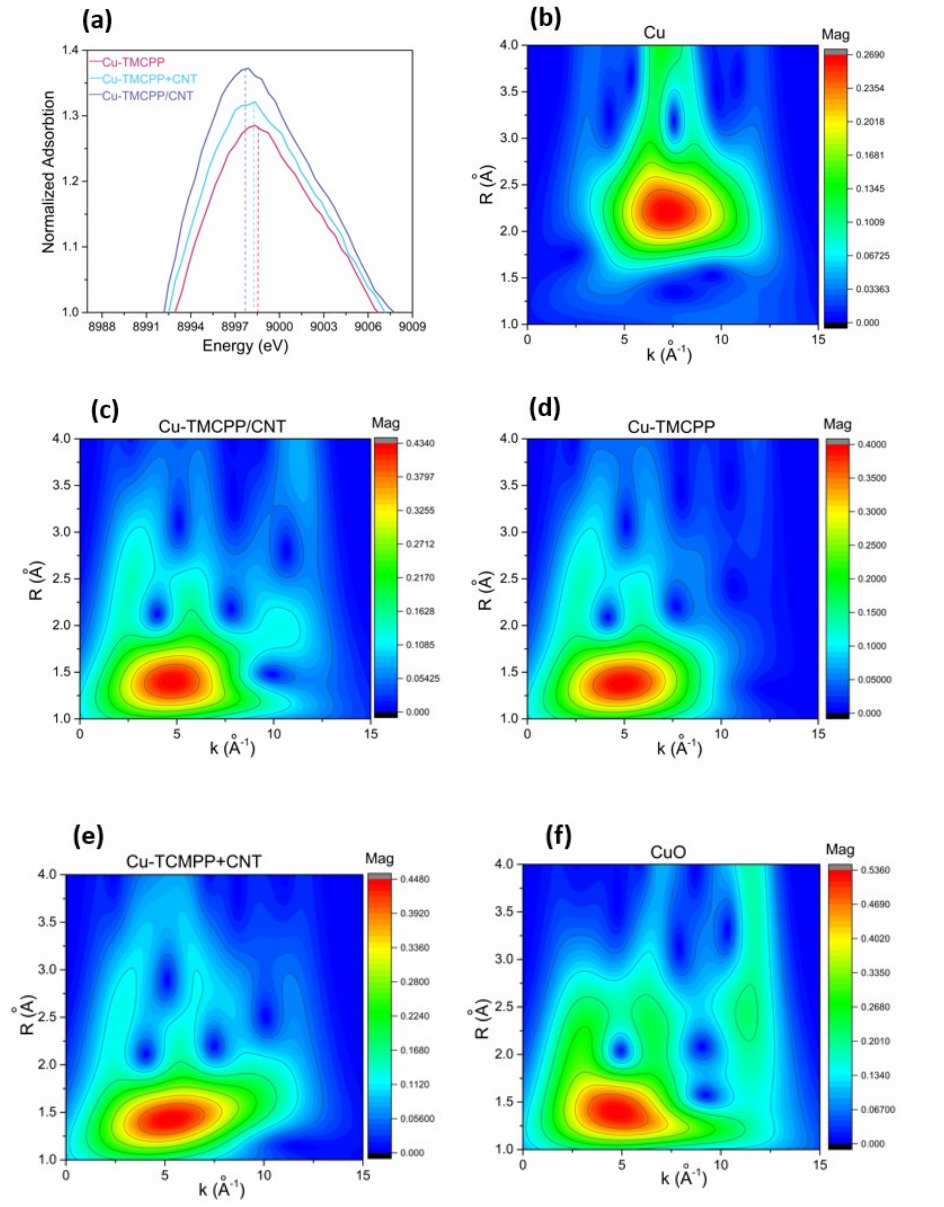

Fig. S4. (a) X-ray Absorption Near Edge Structure (XANES) spectra comparison of Cu-TMCPP/CNT , Cu-TMCPP + CNT and Cu-TMCPP. The wavelet- transform EXAFS (WT-EXAFS) of (b) Cu, (c) Cu-TMCPP/CNT, (d) Cu-TMCPP, (e) Cu-TMCPP + CNT and (f) CuO.

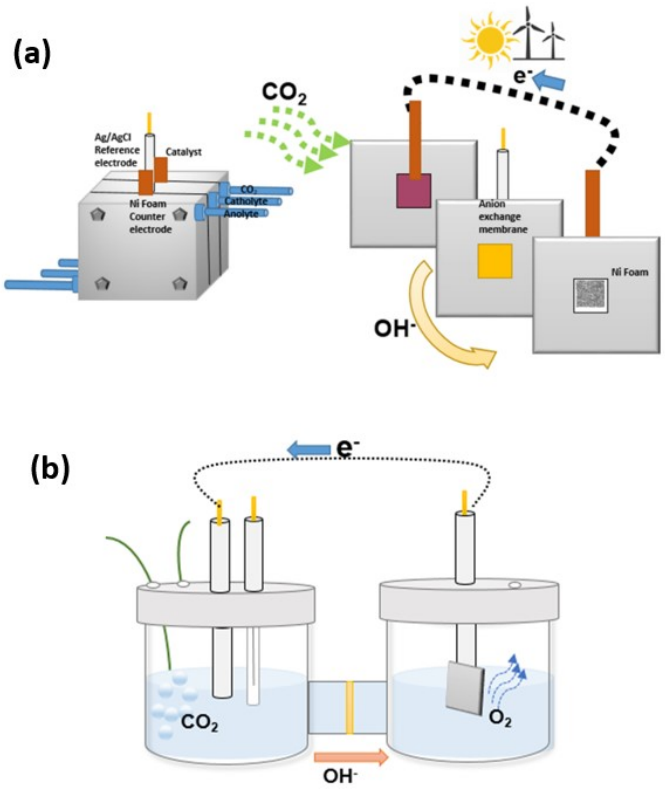

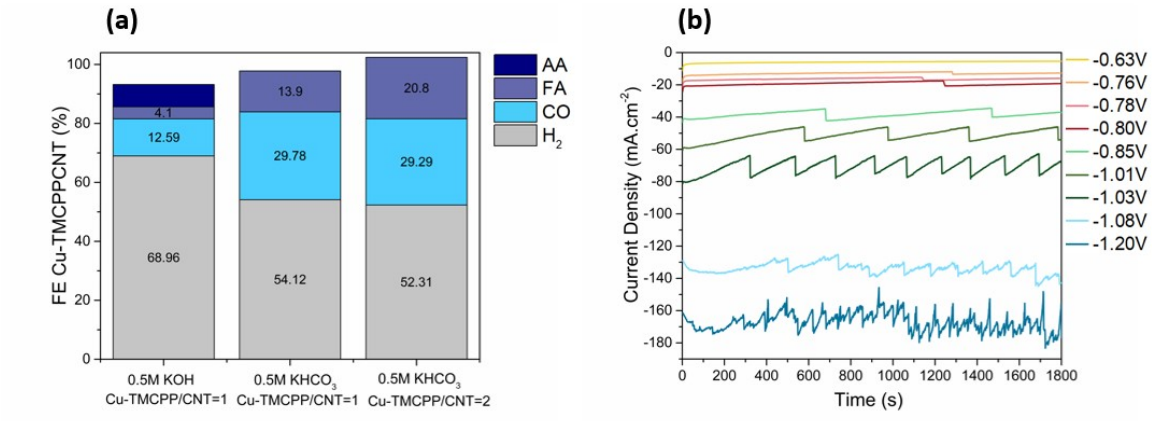

Fig. S5. (a) Flow-cell configuration (b) H-cell configuration.

Fig. S6. (a) for Cu-TMCPP/CNT catalyst, Cu-TMCPP Different loading and different electrolyte at -1V vs RHE were examined, based on the results the catholyte chose to be $KHCO_3$ with less HER (it is worth mentioning that ohmic resistance modification (IR) was not considered in this potential calculation). (b) Chronoamperometry of Cu-TMCPP/CNT under electrocatalytic reaction Conditions of: Working electrode:

Carbon paper gas diffusion layer (GDL); reference electrode: Ag/AgCl; counter electrode: Ni foam in catholyte of 0.5 M $KHCO_3$ and anolyte of 0.5 KOH for 30 min.

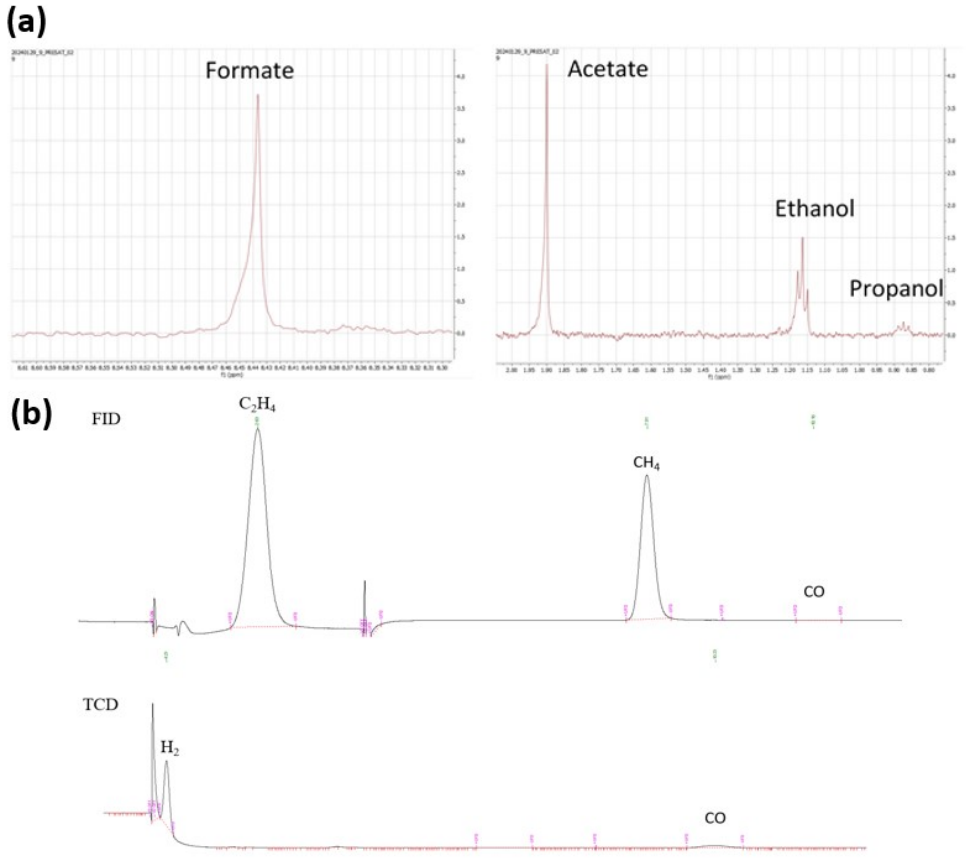

Fig. S7. (a) H-NMR spectrum of liquid product. (b) GC-FID and TCD spectrum.

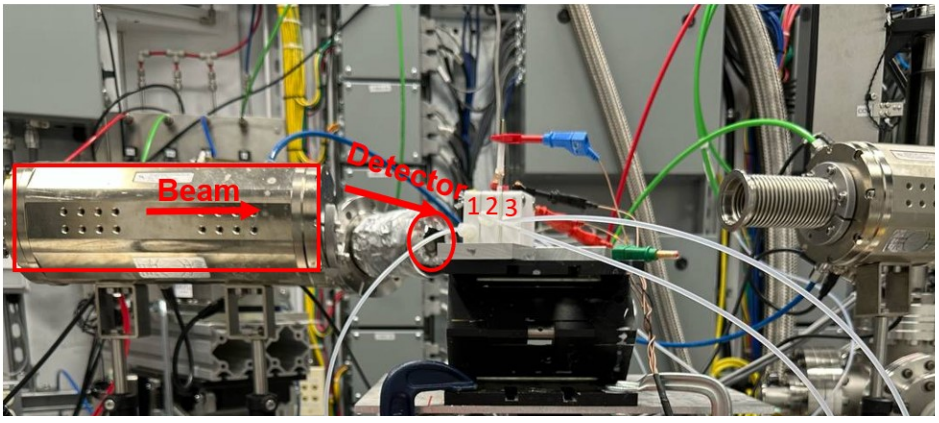

Fig. S8. experimental setup for in-situ XAS measurements. The experiments were performed in a three-chamber flow-cell system: first chamber used for CO_2 purging, second chamber used for catholyte

circulation with carbon paper as the working electrode and third chamber used for Anolyte circulation with Nickel foam as the counter electrode, at the rate of 5 ml min^{-1}.

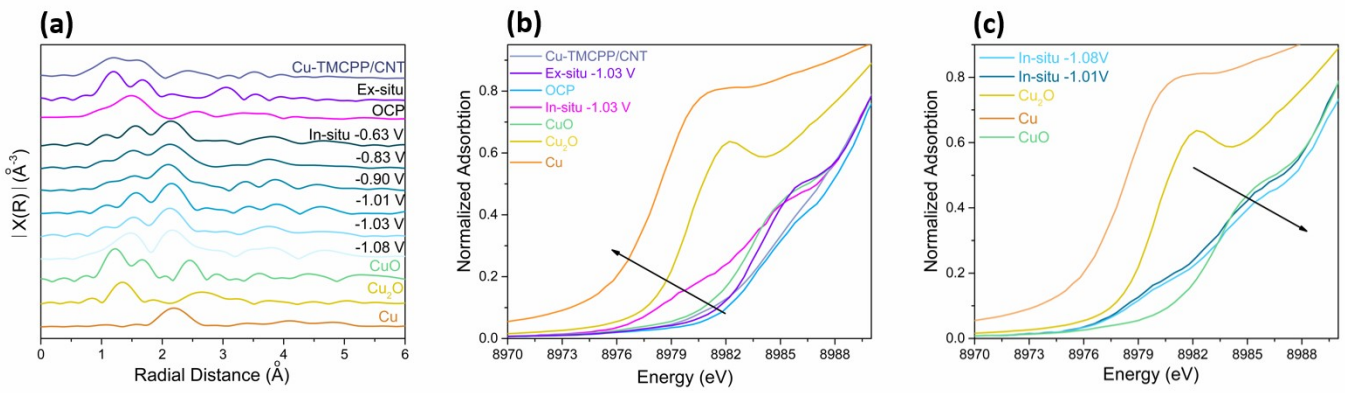

Fig. S9. (a) In-situ Fourier transform EXAFS spectra of Cu-TMCPP/CNT at different potential, and Cu-TMCPP/CNT before and after experiment at -1.03V vs RHE. (b) The XANES spectra at the Cu–K edge at -1.03V vs RHE during and post experiment. (c) The in-situ XANES spectra at the Cu–K edge comparison of -1.01 with -1.08 V vs RHE.

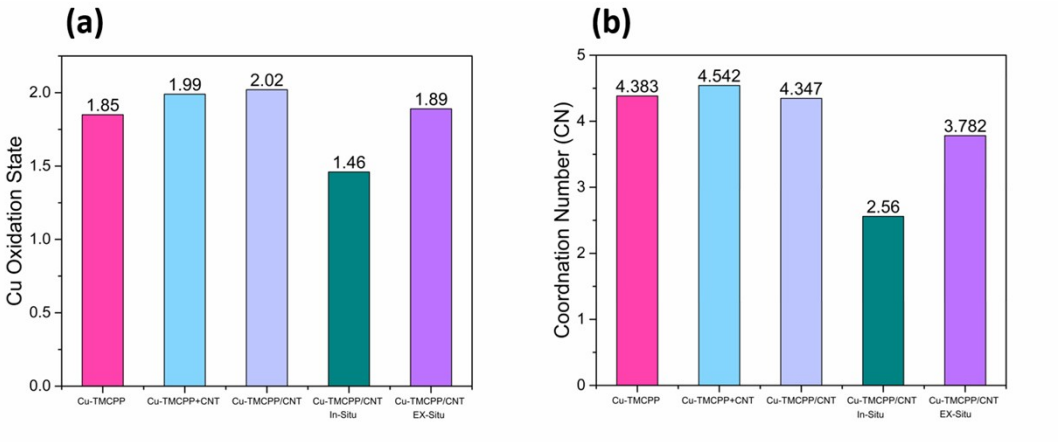

Fig. S10. (a) Oxidation state Cu-TMCPP, Cu-TMCPP + CNT, Cu-TMCPP/CNT before during and after electrocatalytic reaction in flow-cell at -1.03 V vs RHE. (b) Cu coordination number with regard to N of Cu-TMCPP, Cu-TMCPP + CNT, Cu-TMCPP/CNT before during and after electrocatalytic reaction in flow-cell at -1.03 V vs RHE.

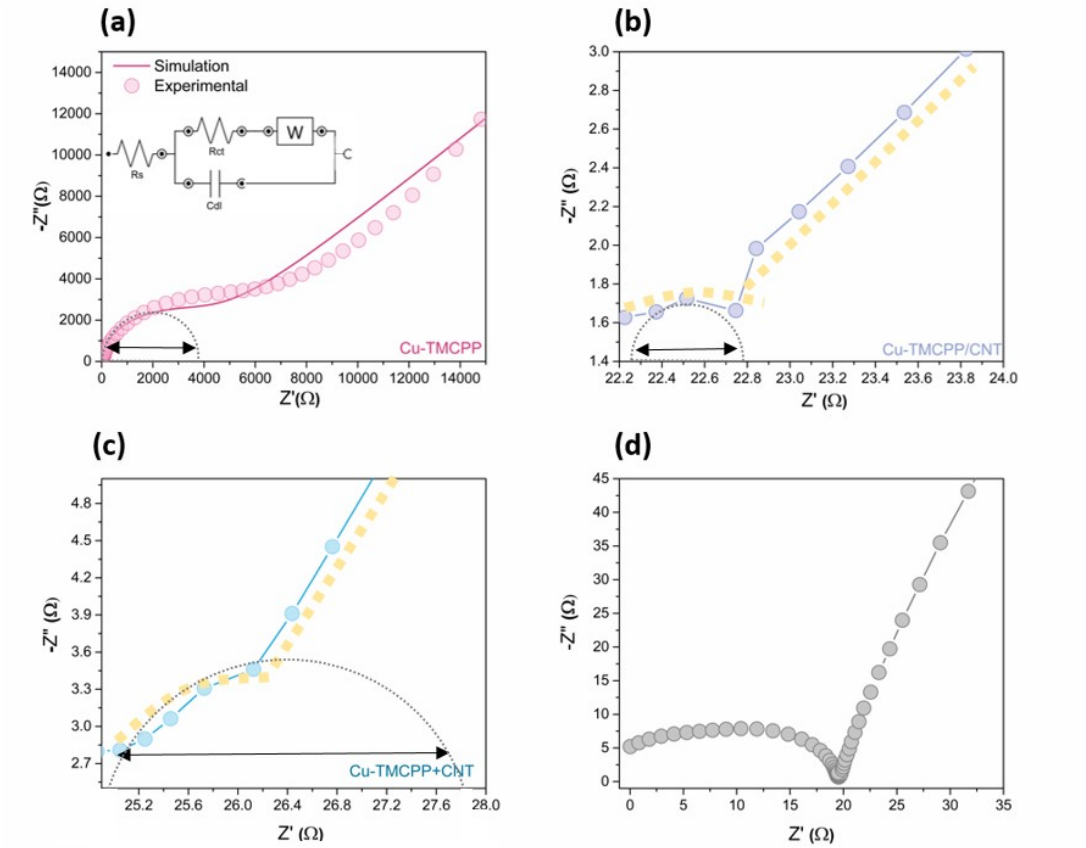

Fig. S11. Nyquist plots of (a) Cu-TMCPP in H- cell with Randles' equivalent circuit. Rs, Cdl, Rct, and Zw stand for the solution resistance, double-layer capacitance, charge-transfer resistance, and Warburg impedance element respectively. Nyquist plots of (b), Cu-TMCPP/CNT and (c) Cu-TMCPP + CNT drop casted on glassy carbon used in H-cell. Nyquist plots of (d) Cu-TMCPP in flow-cell used for IR modification in potential calculation.

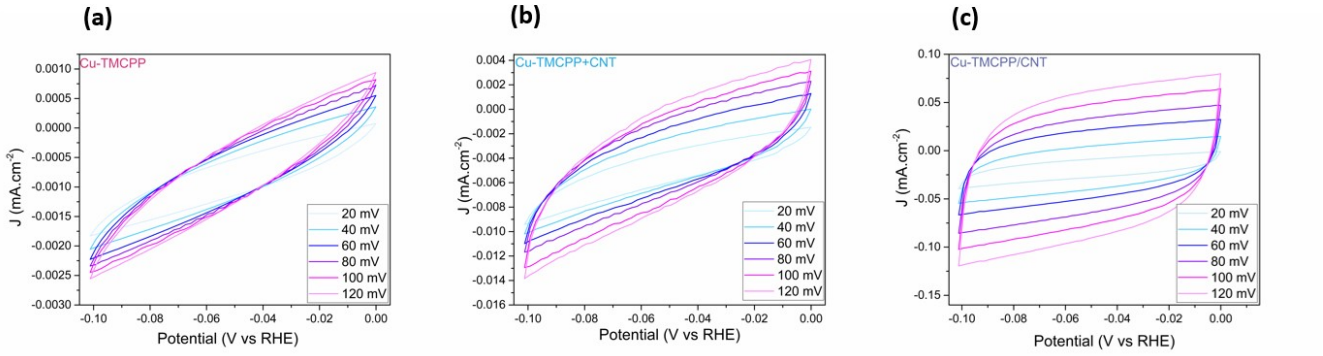

Fig. S12. CV plots in H-cell using working electrode of (a) Cu-TMCPP, (b) Cu-TMCPP + CNT and (c) Cu-TMCPP/ CNT in the non-Faradaic region with various scan rates (20 ~ 120 mV s^{-1}) used for electrochemical double-layer capacitance calculation.

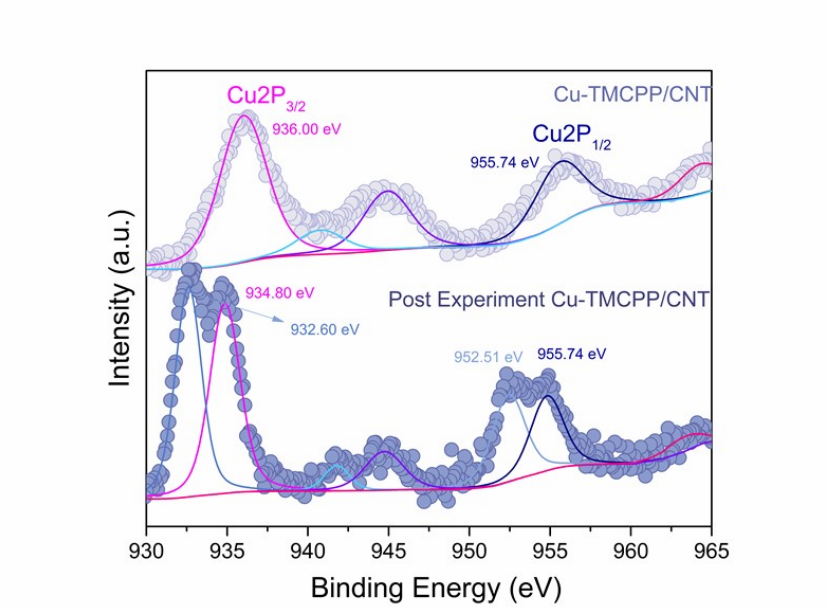

Fig. S13: XPS spectra of Cu 2p in Cu-TMCPP/CNT before and after stability test for 9 h at a constant potential of -1.08 V vs. RHE. The working electrode, a carbon paper gas diffusion layer (GDL); the reference electrode, Ag/AgCl; and the counter electrode, Ni foam. The catholyte, 0.5 M $KHCO_3$; the anolyte, 0.5 M KOH.

Table S1. Cu K-edge EXAFS curve fitting parameters $S0^2$ is the amplitude reduction factor; CN is the coordination number; R is interatomic distance; σ^2 is Debye-Waller factor (a measure of structural disorder).

	Coordination number (CN) Fitting with copper-porphyrin structure Cu- N1	sigma^2(A^o)	Oxidation state	R (A^o)
Cu-TMCPP	4.383	0.00557	1.846	1.94893
Immobilized Cu-TMCPP CNT	4.347	0.00541	2.016	1.97749
Cu-TMCPP CNT mixture	4.542	0.00348	1.987	1.99507
Immobilized Cu-TMCPP CNT AFTER reaction	3.782	0.00362	1.898	1.9561
Immobilized Cu-TMCPP CNT under reaction	2.40	0.00430	1.464	2.01075

Table S2. FE, stability and applied potential (V) reported for Copper porphyrin and phthalocyanine based catalysts.

Porphyrin based Catalyst	FE	Stability	Applied potential (V)	Ref
Cu-TMCPP	CH_4:33.11% H_2 : 56.76%	-	-1.29V vs RHE	This work
Cu-TMCPPCNT I	CH_4:37.28% C_2H_2:13.97% H_2 : 21.5%	7.5 hr	-1.08 V vs RHE	This work
Copper-Porphyrin	CH_4: 56%	-	-1.4 V vs RHE	9
Copper(II)- Porphyrin	CH_4:51.3%	6 hr	1.5 V V vs RHE	10
Copper(ii) tetrakis(pentafluorophenyl)porphyrin	CO: 76.6% H_2 : 1.7%	-	-2.39 V vs. Fc/Fc+	11
Copper-porphyrin complex (copper(II)-5,10,15,20- tetrakis(2,6-dihydroxyphenyl) porphyrin) on polytetrafluoroethylene-treated carbon fiber paper	CO: 12% CH_4: 27%	-	-0.976 V vs RHE	12
Cathodized copper porphyrin metal–organic framework nanosheets	Format: 68.4%	-	-1.55 V vs Ag/Ag^+	13
Cu-Porphyrin- Based Nanosheet	CH_4 :70%	5 hr	-1.6V vs RHE	14
Amino copper porphyrin	CH_4: 54.8%	≈10 h	-1.63 V vs RHE	15
Copper(II) phthalocyanine	CH_4: 66%	-	-1.06 V vs RHE	16
Copper(II) phthalocyanine -CNT	CO:43.9% H_2: 31.3 %	-	-1.05 V vs RHE	17
Cu Porphyrin	CH_4 :55.8%	≈11 h	-1 V vs RHE	18
Porphyrin Framework Coupled with Cu_2O Nanoparticles	C_2H_4 :70.0%	16 h	-1.1 V vs RHE	19

References

1 M. Abdinejad, C. Dao, B. Deng, F. Dinic, O. Voznyy, X. A. Zhang and H. B. Kraatz, *ACS Sustain. Chem. Eng.*, 2020, **8**, 9549–9557.

2 D. Porphyrins, P. Complexes, M. Synthesis and N. P. Complexes, 1–22.

3 Q. Zhu, C. L. Rooney, H. Shema, C. Zeng, J. A. Panetier, E. Gross, H. Wang and L. R. Baker, *Nat. Catal.*, DOI:10.1038/s41929-024-01190-9.

4 M. Abdinejad, C. Dao, B. Deng, M. E. Sweeney, F. Dielmann, X. an Zhang and H. B. Kraatz, *ChemistrySelect*, 2020, **5**, 979–984.

5 W. Nie and C. C. L. McCrory, *Chem. Commun.*, 2018, **54**, 1579–1582.

6 M. Abdinejad, A. Seifitokaldani, C. Dao, E. H. Sargent, X. A. Zhang and H. B. Kraatz, *ACS Appl. Energy Mater.*, 2019, **2**, 1330–1335.

7 R. Giovannetti, *Macro To Nano Spectrosc.*, 2012, 87–109.

8 W. Chen and S. Fukuzumi, *Eur. J. Inorg. Chem.*, 2009, **4**, 5494–5505.

9 Y. Zhou, S. Chen, S. Xi, Z. Wang, P. Deng, F. Yang, Y. Han, Y. Pang and B. Y. Xia, *Cell Reports Phys. Sci.*, 2020, **1**, 100182.

10 Y. Zhang, Q. Zhou, P. Wang, Y. Zhao, F. Gong and W. Y. Sun, *ChemSusChem*, 2022, **15**, 1–7.

11 K. Kosugi, H. Kashima, M. Kondo and S. Masaoka, *Chem. Commun.*, 2022, **58**, 2975–2978.

12 Z. Weng, J. Jiang, Y. Wu, Z. Wu, X. Guo, K. L. Materna, W. Liu, V. S. Batista, G. W. Brudvig and H. Wang, *J. Am. Chem. Soc.*, 2016, **138**, 8076–8079.

13 J. X. Wu, S. Z. Hou, X. Da Zhang, M. Xu, H. F. Yang, P. S. Cao and Z. Y. Gu, *Chem. Sci.*, 2019, **10**, 2199–2205.

14 Y. R. Wang, M. Liu, G. K. Gao, Y. L. Yang, R. X. Yang, H. M. Ding, Y. Chen, S. L. Li and Y. Q. Lan, *Angew. Chemie - Int. Ed.*, 2021, **60**, 21952–21958.

15 P. Yu, X. Lv, Q. Wang, H. Huang, W. Weng, C. Peng, L. Zhang and G. Zheng, *Small*, 2023, **19**, 1–7.

16 Z. Weng, Y. Wu, M. Wang, J. Jiang, K. Yang, S. Huo, X. F. Wang, Q. Ma, G. W. Brudvig, V. S. Batista, Y. Liang, Z. Feng and H. Wang, *Nat. Commun.*, 2018, **9**, 1–9.

17 N. M. Latiff, X. Fu, D. K. Mohamed, A. Veksha, M. Handayani and G. Lisak, *Carbon N. Y.*, 2020, **168**, 245–253.

18 H. Jiang, P. Zhao, H. Shen, S. Yang, R. Gao, Y. Guo, Y. Cao, Q. Zhang and H. Zhang, *Small*, 2024, **20**, 1–9.

19 R. Purbia, S. Y. Choi, C. H. Woo, J. Jeon, C. Lim, D. K. Lee, J. Y. Choi, H. S. Oh and J. M. Baik, *Appl. Catal. B Environ.*, 2024, **345**, 123694.